A smooth model for fiber lay-down processes and its diffusion approximations

M. Herty* A. Klar†‡ S. Motsch § F. Olawsky ‡

Contents

Introduction **2**

1 The new model with smooth trajectories **3**
1.1 White noise limit: connection to the original model 5
1.2 Large diffusion for the original model 7
1.3 Large diffusion limit of the smooth model 7

2 Numerical simulation of the model **12**
2.1 The smooth model for different parameters 12
2.2 Comparison with numerical experiments 13

3 Summary and Conclusions **16**

Appendix **19**

Abstract

In this paper we improve and investigate a stochastic model and its associated Fokker-Planck equation for the lay-down of fibers on a conveyor belt in the production process of nonwoven materials which has been developed in [2]. The model is based on a stochastic differential equation taking into account the motion of the fiber under the influence of turbulence. In the present paper we remove an obvious drawback of the model, namely the non-differentiability of the paths of the process. We develop a model with smoother trajectories and investigate the relations between the different models looking at different scalings and diffusion approximations. Moreover, we compare the numerical results to simulations of the full physical process.

*Fachbereich Mathematik, RWTH Aachen, Germany, {herty@mathc.rwth-aachen.de}
†Fachbereich Mathematik, Technische Universität Kaiserslautern, Germany
‡Fraunhofer ITWM, Kaiserslautern, Germany, {klar@itwm.fhg.de}, {olawsky@itwm.fhg.de}
§Institut Mathématique de Toulouse IMT, Toulouse, France, {motsch@mip.ups-tlse.fr}

Keywords. fiber dynamics, Fokker-Planck equations, diffusion approximation
AMS Classification.

Introduction

Nonwoven materials / fleece are webs of long flexible fibers that are used for composite materials (filters) as well as in the hygiene and textile industries. They are produced in melt-spinning operations: hundreds of individual endless fibers are obtained by the continuous extrusion of a molten polymer through narrow nozzles that are densely and equidistantly placed in a row at a spinning beam. The viscous / viscoelastic fibers are stretched and spun until they solidify due to cooling air streams. Before the elastic fibers lay down on a moving conveyor belt to form a web, they become entangled and form loops due to the highly turbulent air flows. The homogeneity and load capacity of the fiber web are the most important textile properties for quality assessment of industrial nonwoven fabrics. The optimization and control of the fleece quality require modeling and simulation of fiber dynamics and lay-down; in addition, it is necessary to determine the distribution of fiber mass and directional arrangement in the web.

The software FIDYST, developed at the Fraunhofer ITWM, Kaiserslautern, enables numerical simulation of the spinning and deposition regime in the nonwoven production processes. The interaction of the fiber with the turbulent air flows is described by a combination of deterministic and stochastic forces in the momentum equation, which is derived, analyzed and experimentally validated in [8]. Due to the huge amount of physical details incorporated in FIDYST, the simulations of the fiber spinning and lay-down usually require an extremely large computational effort. Hence the optimization and control of the full process with several hundreds of fibres, and of the quality of the fleece, are difficult. Thus, a simplified stochastic model for the fiber lay-down process has been presented in [1, 2]. The model describes the position of the fiber on the transport belt by a stochastic differential system containing parameters that characterize the process. The reduced model can be used to calculate fast and efficiently the performance of hundreds of long fibers for fleece production. The case of large turbulence noise has been investigated in the above papers. In this case the probability density of the fiber becomes rapidly independent of the angle between the fiber and the direction of the conveyor's motion and the angle between the fiber and the position vector of its tip, respectively. In particular, the limit processes turn out to be Ornstein–Uhlenbeck type stochastic processes. Further analytical and numerical investigations can be found in [6, 7].

Although this model describes already several features of the full physical process correctly, it has an obvious drawback, namely the non-differentiability of the paths of the process. This is not true for the physical process and can also be seen, comparing simulation results of the full physical model and of the simplified model

explained above, see Section 2.2. Thus, the purpose of the present paper is to develop a model with smoother trajectories, compare the results with the full process and investigate the relations of this new model with the model described above and its simplifications.

The outline of the paper is as follows: In Section 1, we introduce the new model and we investigate different scalings leading to the original model and to the reduce model. In section 2, we explore numerical simulation of the smooth model with different scales which illustrate the results of Section 1. We also compare the numerical simulation with the full physical model.

1 The new model with smooth trajectories

In the following we describe the original model in more detail. Consider a slender, elastic, non-extensible and endless fiber in a lay-down regime. The motion of the fiber on the belt is parameterized by its position $\vec{x}(t)$ and its velocity $c\vec{\tau}(\alpha)$, where c is the magnitude of the velocity:

$$\vec{\tau}(\alpha) = \begin{pmatrix} \cos\alpha \\ \sin\alpha \end{pmatrix}$$

and α is the angle between the x-axis and the vector speed (see figure 1). Choosing arc-length parameterization, the non-extensibility condition gives $c = 1$. With $\vec{\tau}^{\perp}(\alpha) = (-\sin\alpha, \cos\alpha)^T$ the original model [1, 2] for the process is given by

$$\begin{aligned} d\vec{x}_t &= \vec{\tau}(\alpha_t)\, dt, \\ d\alpha_t &= -b(|\vec{x}_t|)\frac{\vec{x}_t}{|\vec{x}_t|} \cdot \vec{\tau}^{\perp}(\alpha_t)\, dt + A dW_t. \end{aligned} \tag{1}$$

The function b denotes the effect of an external force which makes the fiber goes back to the origin, AdW_t express the stochasticity of the system due to the airflow. Another way to see the effect of the force is to look at the system in polar coordinates. Let's define $\vec{x} = r\vec{\tau}(\phi)$ then the force can be expressed as :

$$\begin{aligned} -b(|\vec{x}|)\frac{\vec{x}}{|\vec{x}|} \cdot \vec{\tau}^{\perp}(\alpha) &= -b(r)\vec{\tau}(\phi) \cdot \vec{\tau}^{\perp}(\alpha) \\ &= -b(r)\left(-\cos\phi\, \sin\alpha + \sin\phi\, \cos\alpha\right) \\ &= -b(r)\sin(\phi - \alpha) \end{aligned}$$

I.e. another form of the model is :

$$\begin{aligned} d\vec{x}_t &= \vec{\tau}(\alpha_t)\, dt, \\ d\alpha_t &= b(r_t)\sin(\pi + \phi_t - \alpha_t)\, dt + A dW_t. \end{aligned} \tag{2}$$

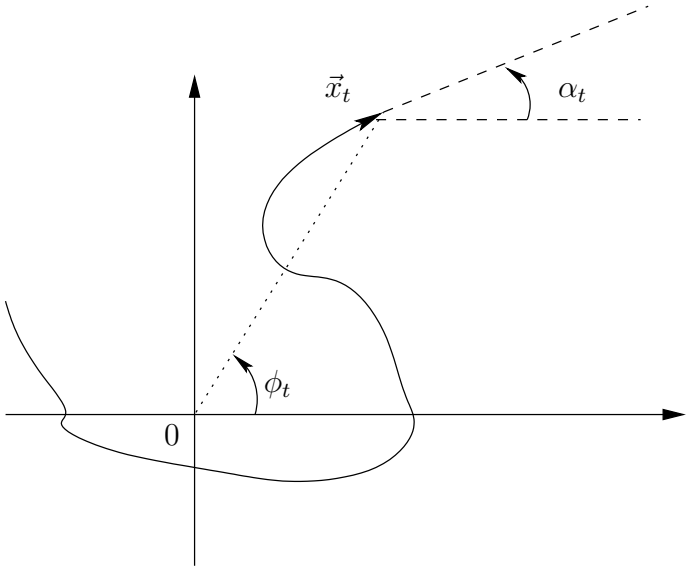

Figure 1: The description of the fiber process.

The equation on α express the fact that α is going to relax to $\pi + \phi$ which is the direction of the origin at the position $\vec{x}$.

For large value of noise A, we will see that the dynamic of equation (2) could be reduced to the simple equation

$$d\vec{x}_t = -\frac{1}{A^2}\frac{b(|\vec{x}_t|)}{|\vec{x}_t|}\vec{x}_t dt + \frac{\sqrt{2}}{A}dW_t. \tag{3}$$

(see Section 1.2). We call equation (2) the reduced model.

In order to get smoother fiber trajectories, we change the original model (1). To this aim, we add the white noise term in the differential equation not on the level of the velocity equation but on the second derivative, the curvature. We propose the following model:

$$\begin{aligned} d\vec{x}_t &= \vec{\tau}(\alpha_t)\, dt \\ d\alpha_t &= \kappa_t\, dt \\ d\kappa_t &= \lambda(\kappa_0 - \kappa)\, dt + \mu dW_t, \end{aligned} \tag{4}$$

where $\kappa_0(\vec{x}_t, \alpha_t) = b(r_t)\sin(\alpha_t - \phi)$. Here, the new parameter λ describes the inverse stiffness of the fiber and is related to the inverse elasticity module. The smaller λ the stiffer is the fiber. μ or better $\frac{\mu}{\lambda}$ describes the influence of the turbulent airflow on the curvature.

In the next subsection (Section 1.1), we are going to prove that the smooth model given by equation (4) leads to the original model (1) in a certain asymptotic scaling. Combining this with the large noise asymptotic (Section 1.2), one can jump

from the smooth model to the original model and then to the reduced model (2). In the last subsection (Section 1.3), we will directly derive the reduced model (3) from the smooth model (4) with another asymptotic.

1.1 White noise limit: connection to the original model

In this part, we are going to prove that the smooth model leads under the appropriate scaling to the original model.

Proposition 1.1 *The following rescaling for equation (4):*

$$\lambda' = \varepsilon^2 \lambda \quad ; \quad \mu' = \varepsilon^2 \mu \tag{5}$$

together with a rescaling of the curvature

$$\kappa' = \varepsilon \kappa \tag{6}$$

leads to the original model (1) with the diffusion coefficient $A = \frac{\mu}{\lambda}$.

Proof. If we insert the rescaling given by (5) into the smooth model for the fiber, we obtain :

$$\begin{aligned} d\vec{x}_t &= \vec{\tau}(\alpha_t)\, dt \\ d\alpha_t &= \kappa_t\, dt \\ d\kappa_t &= \frac{\lambda'}{\varepsilon^2}(\kappa_0 - \kappa)\, dt + \frac{\mu'}{\varepsilon^2} dW_t \end{aligned}$$

To facilitate the reading, we drop off the tilde. If we want to look at the limit when ε goes to zero, we have to make a change of variable for the κ-variable:

$$\kappa' = \varepsilon \kappa.$$

The dynamics for the fiber are then described by

$$\begin{aligned} d\vec{x}_t &= \vec{\tau}(\alpha_t)\, dt \\ d\alpha_t &= \frac{1}{\varepsilon}\kappa_t\, dt \\ d\kappa_t &= \frac{\lambda}{\varepsilon^2}(\varepsilon\kappa_0\, dt - \kappa)\, dt + \frac{\mu}{\varepsilon} dW_t \end{aligned}$$

The equations for α and κ describe a process of Ornstein–Uhlenbeck type, the above scaling is the so called White-noise scaling of the Ornstein–Uhlenbeck process, see e.g. [4]. In terms of the Fokker-Planck equation, this gives after multiplication with ε

$$\partial_t f^\varepsilon + \vec{\tau}(\alpha) \cdot \nabla_{\vec{x}} f^\varepsilon + \frac{1}{\varepsilon}\left(\kappa \partial_\alpha f^\varepsilon + \lambda \kappa_0 \partial_\kappa f^\varepsilon\right) = \frac{1}{\varepsilon^2}\left(\lambda \partial_\kappa (\kappa f^\varepsilon) + \frac{\mu^2}{2} \partial_{\kappa^2} f^\varepsilon\right) \tag{7}$$

We use an Hilbert expansion for f^ε ($f^\varepsilon = f^0 + \varepsilon f^1 + \dots$) in order to find the limit equation as ε goes to zero. At order ε^{-1}, we have :

$$\varepsilon^{-1} \quad : \quad \lambda \partial_\kappa(\kappa f^0) + \frac{\mu^2}{2}\partial_{\kappa^2} f^0 = 0.$$

This equation implies that f^0 is Gaussian in κ-variable. More exactly, if we define $p^\varepsilon = \int_\kappa f^\varepsilon \, d\kappa$, we then could write :

$$f^0 = p^0(\vec{x}, \alpha) \frac{1}{\sqrt{\pi \mu^2/\lambda}} \mathrm{e}^{-\frac{\kappa^2}{\mu^2/\lambda}}.$$

At the order ε^0 in equation (7), we have :

$$\varepsilon^0 \quad : \quad \kappa \partial_\alpha f^0 + \lambda \kappa_0 \partial_\kappa f^0 = \lambda \partial_\kappa(\kappa f^1) + \frac{\mu^2}{2}\partial_{\kappa^2} f^1.$$

Although an explicit expression for f^1 is not available, we can integrate this equation against κ. This gives :

$$\frac{\mu^2}{2\lambda}\partial_\alpha p_0 - \lambda \kappa_0 \, p_0 = -\lambda \int_\kappa \kappa f^1 \, d\kappa.$$

Now we go back to the original equation on f^ε and we integrate in κ :

$$\varepsilon(\partial_t p^\varepsilon + \vec{\tau}(\alpha) \cdot \nabla_{\vec{x}} p^\varepsilon) + \partial_\alpha \int_\kappa \kappa f^\varepsilon \, d\kappa + 0 = 0,$$

But now we can compute the integral at order 1 :

$$\begin{aligned} \int_\kappa \kappa f^\varepsilon \, d\kappa &= \int_\kappa \kappa (f^0 + \varepsilon f^1) \, d\kappa + O(\varepsilon^2) \\ &= 0 + \varepsilon \int_\kappa \kappa f^1 \, d\kappa + O(\varepsilon^2) \\ &= \varepsilon \left(\kappa_0 \, p_0 - \frac{\mu^2}{2\lambda^2}\partial_\alpha p_0 \right) + O(\varepsilon^2). \end{aligned}$$

So finally we have at the limit $\varepsilon \to 0$:

$$\partial_t p^0 + \vec{\tau}(\alpha) \cdot \nabla_{\vec{x}} p^0 + \partial_\alpha(\kappa_0 p_0) = \frac{\mu^2}{2\lambda^2}\partial_{\alpha^2} p_0.$$

We recover our initial Fokker-Planck equation for the fiber-process with $A = \frac{\mu}{\lambda}$. $\square$

1.2 Large diffusion for the original model

Now we connect the original model with the reduced model looking at the large noise regime in the equation:

$$\begin{aligned} d\vec{x}_t &= \vec{\tau}(\alpha_t)\, dt, \\ d\alpha_t &= b(r_t)\sin(\alpha_t - \phi_t)\, dt + A dW_t. \end{aligned}$$

Since the proof is very similar to the previous one (proposition 1.1), we defer the proof in the appendix. See also [2] for another proof.

Proposition 1.2 *Considering the dynamics given by equation (1) and the rescaling*

$$t' = \varepsilon t \quad , \quad A' = \sqrt{\varepsilon} A \tag{8}$$

leads to the reduced equations

$$d\vec{x}_t = -\frac{1}{A^2} b(r_t)\vec{\tau}(\phi_t) dt + \frac{\sqrt{2}}{A} dW_t,$$

or

$$d\vec{x}_t = -\frac{1}{A^2}\frac{b(|\vec{x}_t|)}{|\vec{x}_t|}\vec{x}_t dt + \frac{\sqrt{2}}{A} dW_t. \tag{9}$$

In terms of the density distribution $n(t, \vec{x})$ the Fokker-Planck equation reads:

$$\partial_t n - \frac{1}{A^2}\nabla_{\vec{x}} \cdot (b(r)\vec{\tau}(\phi)\, n) = \frac{1}{A^2}\Delta_{\vec{x}} n \tag{10}$$

1.3 Large diffusion limit of the smooth model

In this Section, we derive the reduced model (3) directly from the smooth model (4).

Proposition 1.3 *The following rescaling for the dynamic given by equation (4) :*

$$\lambda' = \varepsilon\lambda \quad ; \quad \mu' = \varepsilon^{3/2}\mu \tag{11}$$

together with a rescaling of time and curvature

$$t' = \varepsilon t \quad ; \quad \kappa' = \varepsilon\kappa \tag{12}$$

lead to a reduced model of the form

$$\partial_t n^0 - \frac{\lambda^2}{\mu^2}\nabla_{\vec{x}} \cdot \left(\vec{\tau}(\phi) b(r) n^0\right) = \frac{1}{2\lambda} D(\frac{\mu^2}{2\lambda^3})\Delta_{\vec{x}} n^0, \tag{13}$$

Proof. As for the proof of proposition 1.1, we have to rescale κ if we want to find a limit when ε goes to zero. Once again, we use :

$$\kappa' = \varepsilon\kappa.$$

Therefore, using (11) the equation for the fiber is :

$$\begin{aligned} d\vec{x}_t &= \vec{\tau}(\alpha_t)\, dt \\ d\alpha_t &= \frac{1}{\varepsilon}\kappa_t\, dt \\ d\kappa_t &= \frac{\lambda'}{\varepsilon}(\varepsilon\kappa_0 - \kappa)\, dt + \frac{\mu'}{\sqrt{\varepsilon}} dW_t. \end{aligned}$$

The associated Fokker-Planck equation is after the time rescale:

$$\varepsilon\partial_t f^\varepsilon + \vec{\tau}(\alpha)\cdot\nabla_{\vec{x}} f^\varepsilon + \lambda\kappa_0\partial_\kappa f^\varepsilon = \frac{1}{\varepsilon}\left(-\kappa\partial_\alpha f^\varepsilon + \lambda\partial_\kappa(\kappa f^\varepsilon) + \frac{\mu^2}{2}\partial_{\kappa^2} f^\varepsilon\right). \qquad (14)$$

Let's denote by Q the operator on the right-hand side :

$$Q(f) = -\kappa\partial_\alpha f + \lambda\partial_\kappa(\kappa f) + \frac{\mu^2}{2}\partial_{\kappa^2} f.$$

Making an Hilbert expansion for f^ε, we have at order ε^{-1} :

$$\varepsilon^{-1} \quad : \quad Q(f) = 0.$$

This equation is solved by :

$$f^0 = n^0(t,\vec{x})\,\frac{M(\kappa)}{2\pi},$$

where $M(\kappa)$ is a Gaussian with mean zero and variance $\frac{\mu^2}{2\lambda}$.
At order ε^0, we have :

$$\varepsilon^0 \quad : \quad \vec{\tau}(\alpha)\cdot\nabla_{\vec{x}} f^0 + \lambda\kappa_0\partial_\kappa f^0 = Q(f^1).$$

This equation could not be solved explicitly for f^1. But since the equation is linear and only involved (α,κ) variable which is decoupled in f^0, we can express f^1 as :

$$f^1 = \vec{\chi}_1\cdot\nabla_{\vec{x}} n^0 \;+\; b(r)n^0\vec{\chi}_2\cdot\begin{pmatrix} -\sin\phi \\ \cos\phi \end{pmatrix}$$

where $\vec{\chi}_1(\alpha,\kappa)$ and $\vec{\chi}_2(\alpha,\kappa)$ satisfy :

$$\vec{\tau}(\alpha)\frac{M}{2\pi} = Q(\vec{\chi}_1) \qquad (15)$$

$$\lambda\vec{\tau}(\alpha)\partial_\kappa\left(\frac{M}{2\pi}\right) = Q(\vec{\chi}_2). \qquad (16)$$

Now we can look at the order ε^1. We first integrate equation (14) over (α, κ), this gives :

$$\partial_t n^\varepsilon + \nabla_{\vec{x}} \cdot J^\varepsilon = 0, \tag{17}$$

with :

$$J^\varepsilon = \frac{1}{\varepsilon} \int_{\alpha,\kappa} \vec{\tau}(\alpha) f^\varepsilon \, d\alpha d\kappa.$$

The smaller λ the stiffer is the fiber.

Using the Hilbert expansion on f^ε, we then have :

$$\begin{aligned} J^\varepsilon &= 0 + \int_{\alpha,\kappa} \vec{\tau}(\alpha) f^1 \, d\alpha d\kappa + O(\varepsilon) \\ &= \int_{\alpha,\kappa} \vec{\tau}(\alpha) \left(\vec{\chi}_1 \cdot \nabla_{\vec{x}} n^0 \; + \; b(r) n^0 \, \vec{\chi}_2 \cdot \begin{pmatrix} -\sin\phi \\ \cos\phi \end{pmatrix} \right) d\alpha d\kappa \\ &= -A_1 \nabla_{\vec{x}} n^0 \; - \; A_2 \begin{pmatrix} -\sin\phi \\ \cos\phi \end{pmatrix} b(r) n^0 \; + \; O(\varepsilon), \end{aligned}$$

with :

$$A_1 = -\int_{\alpha,\kappa} \vec{\tau}(\alpha) \otimes \vec{\chi}_1 \, d\alpha d\kappa \tag{18}$$

$$A_2 = -\int_{\alpha,\kappa} \vec{\tau}(\alpha) \otimes \vec{\chi}_2 \, d\alpha d\kappa. \tag{19}$$

Finally, we replace J^ε by this last expression in equation (17) :

$$\partial_t n^\varepsilon + \nabla_{\vec{x}} \cdot \left(-A_1 \nabla_{\vec{x}} n^0 \; - \; A_2 \begin{pmatrix} -\sin\phi \\ \cos\phi \end{pmatrix} b(r) n^0 \right) = O(\varepsilon).$$

At the limit ε goes to zero, we have :

$$\partial_t n^0 - \nabla_{\vec{x}} \cdot \left(A_2 \begin{pmatrix} -\sin\phi \\ \cos\phi \end{pmatrix} b(r) n^0 \right) = \nabla_{\vec{x}} \cdot \left(A_1 \nabla_{\vec{x}} n^0 \right). \tag{20}$$

To end the proof, we have to calculate the two tensors A_1, A_2. We give the result as a lemma :

Lemma 1.4 *The two tensors A_1 and A_2 given by equation (18) and equation (19) respectively are equal to :*

$$A_1 = \frac{1}{2\lambda} \mathcal{D}\left(\frac{\mu^2}{2\lambda^3}\right) Id_2 \qquad , \qquad A_2 = \frac{\lambda^2}{\mu^2} \begin{bmatrix} 0 & -1 \\ 1 & 0 \end{bmatrix},$$

where : $\mathcal{D}(\alpha^2) = \int_0^\infty \exp\left(-\alpha^2(-1 + s + \mathrm{e}^{-s})\right) ds$ and Id_2 is the identity tensor in $\mathbb{R}^2$.

Using this lemma, we have :

$$\partial_t n^0 - \frac{\lambda^2}{\mu^2}\nabla_{\vec{x}} \cdot \left(\vec{\tau}(\phi) b(r) n^0\right) = \frac{1}{2\lambda}\mathcal{D}(\frac{\mu^2}{2\lambda^3})\Delta_{\vec{x}} n^0, \tag{21}$$

which ends the proof. □

Proof Lemma 1.4. To compute the tensor A_1, we use the result established in [3] which we summarize here : let $\widetilde{\chi}$ be the solution of

$$\vec{\tau}(\alpha)\frac{M_\sigma}{2\pi} = \kappa\partial_\theta\widetilde{\chi} + \partial_\kappa(\kappa\widetilde{\chi}) + \sigma^2\partial_{\kappa^2}\widetilde{\chi}, \tag{22}$$

with M_σ the Gaussian with mean zero and variance σ^2. Then we have :

$$-\int_{\alpha,\kappa} \vec{\tau}(\alpha)\otimes\widetilde{\chi}\, d\alpha d\kappa = \frac{\mathcal{D}(\sigma^2)}{2}\,\mathrm{Id}_2, \tag{23}$$

where $\mathcal{D}(\sigma^2) = \int_0^\infty \exp\left(-\sigma^2(-1+s+\mathrm{e}^{-s})\right)\, ds$.

We want to express $\vec{\chi}_1$ (solution of equation (15)) with $\widetilde{\chi}$. In this aim, we make the change of unknowns $\lambda\kappa' = \kappa$ in (18). The Gaussian M is then transformed as

$$M(\kappa') = \frac{1}{\sqrt{2\pi\mu^2/2\lambda}}\,\mathrm{e}^{-\frac{\kappa^2/\lambda^2}{2\mu^2/2\lambda}} = \frac{1}{\lambda}M'(\kappa'),$$

where M' is a Gaussian with mean zero and variance $\mu^2/2\lambda^3$. With the notation $\vec{\chi'}_1 = \vec{\chi}_1(\alpha,\lambda\kappa)$, the full equation (18) is written

$$\vec{\tau}(\alpha)\frac{1}{\lambda}\frac{M'}{2\pi} = \lambda\kappa'\partial_\theta\vec{\chi'}_1 + \lambda\partial_{\kappa'}(\kappa'\vec{\chi'}_1) + \frac{\mu^2}{2\lambda^2}\,\partial_{\kappa^2}\vec{\chi'}_1$$

or again

$$\vec{\tau}(\alpha)\frac{1}{\lambda^2}\frac{M'}{2\pi} = \kappa'\partial_\theta\vec{\chi'}_1 + \partial_{\kappa'}(\kappa'\vec{\chi'}_1) + \frac{\mu^2}{2\lambda^3}\,\partial_{\kappa^2}\vec{\chi'}_1.$$

Therefore, we have $\vec{\chi'}_1 = \frac{1}{\lambda^2}\,\widetilde{\chi}$, with $\widetilde{\chi}$ the solution of (22) with $\sigma^2 = \frac{\mu^2}{2\lambda^3}$. Now we can compute the tensor A_1 using the change of unknowns $\lambda\kappa' = \kappa$:

$$\begin{aligned} A_1 &= -\int_{\alpha,\kappa}\vec{\tau}(\alpha)\otimes\vec{\chi}_1\, d\alpha d\kappa = -\int_{\alpha,\kappa'}\vec{\tau}(\alpha)\otimes\vec{\chi'}_1\,\lambda\, d\alpha d\kappa' \\ &= -\int_{\alpha,\kappa'}\vec{\tau}(\alpha)\otimes\frac{1}{\lambda^2}\,\widetilde{\chi}\,\lambda\, d\alpha d\kappa' = \frac{1}{\lambda}\,\frac{\mathcal{D}(\frac{\mu^2}{2\lambda^3})}{2}\,\mathrm{Id}_2, \end{aligned}$$

using the result of equation (23).

The calculus of the tensor A_2 is simpler since we can find explicitly a solution to equation (16) :

$$\vec{\chi}_2 = -\frac{2\lambda^2}{\mu^2}\begin{pmatrix}\sin\theta\\ -\cos\theta\end{pmatrix}\frac{M}{2\pi}$$

as we have :

$$\begin{aligned} Q(\vec{\chi}_2) &= \kappa\partial_\theta\vec{\chi}_2 + 0 = -\frac{2\lambda^2}{\mu^2}\kappa\begin{pmatrix}\cos\theta\\ \sin\theta\end{pmatrix}\frac{M}{2\pi} \\ &= \lambda\vec{\tau}(\phi)\partial_\kappa\left(\frac{M}{2\pi}\right). \end{aligned}$$

Therefore the computation of A_2 is straightforward :

$$\begin{aligned} A_2 &= -\int_{\alpha,\kappa}\vec{\tau}(\alpha)\otimes\left(-\frac{2\lambda^2}{\mu^2}\begin{pmatrix}\sin\theta\\ -\cos\theta\end{pmatrix}\frac{M}{2\pi}\right)d\alpha d\kappa. \\ &= \frac{2\lambda^2}{\mu^2}\int_{\alpha,\kappa}\begin{bmatrix}\cos\theta\,\sin\theta & -\cos^2\theta\\ \sin^2\theta & -\sin\theta\,\cos\theta\end{bmatrix}\frac{M}{2\pi}\,d\theta d\kappa \\ &= \frac{\lambda^2}{\mu^2}\begin{bmatrix}0 & -1\\ 1 & 0\end{bmatrix}. \end{aligned}$$

□

Remark. Obviously the limit equations obtained in Lemma 1.3 are not exactly the reduced model (3) obtained in Section 1.1. However, also the scaling used in this section is still not equivalent to the combination of the scalings used in Sections 1.1. Compared to a combination of these scalings we have to rescale the coefficients λ and μ in this section once more using

$$\lambda' = \varepsilon\lambda, \quad \mu' = \varepsilon\mu$$

This leads to a constant value of $\frac{\lambda^2}{\mu^2}$ and a scaled value

$$\frac{\varepsilon}{2\lambda}\mathcal{D}(\frac{\mu^2\varepsilon}{2\lambda^3})$$

for the diffusion coefficient. According to [3] we have the following asymptotic for $\mathcal{D}$:

$$\mathcal{D}(\sigma^2) \overset{\sigma^2\to 0}{\sim} \frac{1}{\sigma^2}.$$

Therefore since $\frac{\mu^2\varepsilon}{2\lambda^3}$ goes to 0 as ε goes to 0, the diffusive coefficient behaves like :

$$\frac{\varepsilon}{2\lambda}D(\frac{\mu^2\varepsilon}{2\lambda^3}) \sim \frac{1}{2\lambda}\frac{2\lambda^3}{\mu^2} = \frac{\lambda^2}{\mu^2},$$

which is exactly the diffusive coefficient we have obtained by making the big noise limit in two steps from the smooth model to the original one and then from the original model to the reduced model.

Remark. (Overview over models and scalings)

The three models discussed in this paper are

Smooth	**Original**	**Reduced**
$d\vec{x}_t = \vec{\tau}(\alpha_t)\,dt$	$d\vec{x}_t = \vec{\tau}(\alpha_t)\,dt$	$d\vec{x}_t = -a_1 b(r)\vec{\tau}(\phi)dt + a_2 dW_t$
$d\alpha_t = \kappa_t\,dt$	$d\alpha_t = \kappa_0\,dt + A dW_t$	
$d\kappa_t = \lambda(\kappa_0 - \kappa)\,dt + \mu dW_t$		

where

$$\kappa_0 = b(r)\sin(\pi + \phi - \alpha_t), \vec{x} = r\vec{\tau}(\phi). \tag{24}$$

The links between them are shown in Figure (2).

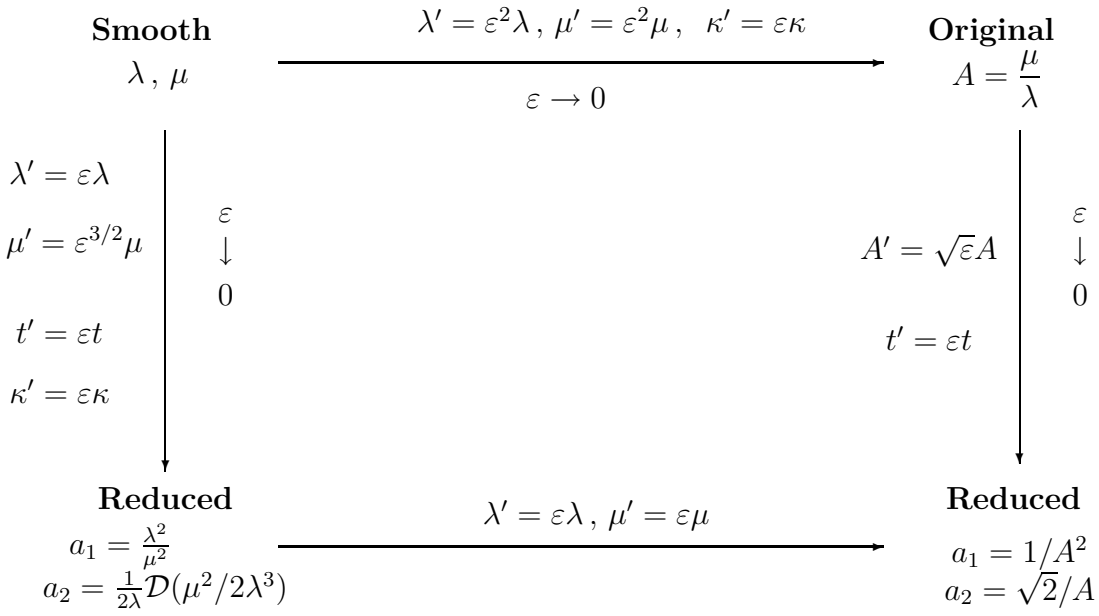

Figure 2: Diagram of the different scaling limits

2 Numerical simulation of the model

2.1 The smooth model for different parameters

In this section we investigate the smooth model numerically. In particular, small and large values of the two parameters, λ related to the inverse elasticity module and turbulence amplitude $A = \frac{\mu}{\lambda}$ are investigated.

We first have to developp a numerical scheme to approximate the solution of the smooth model (eq. 4). All we have to to is to find an accurate scheme for the

evolution of the curvature κ. After that we simply have to integrate in order to have the speed $\vec{\tau}(\theta)$ and the position $\vec{x}$ of the fiber.

A method to solve the equation on the curvature is simply to use an Euler scheme (see [5]). But since this equation is an Ornstein–Uhlenbeck process, we can use a more accurate method. Integrating the quantity $d(\mathrm{e}^{\lambda t}\kappa_t)$, we have the explicit expression:

$$\kappa_t = \mathrm{e}^{-\lambda t}\kappa_0 + \lambda \mathrm{e}^{\lambda t}\int_0^t \kappa_0(s)\mathrm{e}^{\lambda s}\,ds + \mu \mathrm{e}^{-\lambda t}\int_0^t \mathrm{e}^{\lambda s}\,dB_s$$

Denoting by Δt the time step of our numerical scheme, this formulation lead at first order to the algorithm:

$$\kappa_{t_{n+1}} = \mathrm{e}^{-\lambda\Delta t}\kappa_{t_n} + (1-\mathrm{e}^{-\lambda\Delta t})\kappa_0(t_n) + G_{t_n}$$

where κ_{t_n} is the curvature at time t_n, κ_0 is the effect of the external force (eq. 24), G_n is a Gaussian random variable independant of κ_{t_n} with mean 0 and variance $\frac{\mu^2}{\lambda}(1-\mathrm{e}^{-2\lambda\Delta t})$.

After computing the new value of the curvature κ_{t_n}, we simply integrate to update the angle speed and the position using the trapezoidal rule:

$$\begin{aligned}
\theta_{t_{n+1}} &= \theta_{t_n} + \Delta t\,\frac{\kappa_{t_n}+\kappa_{t_{n+1}}}{2} \\
\vec{x}_{t_{n+1}} &= \vec{x}_{t_n} + \Delta t\,\frac{\vec{\tau}(\theta_{t_n})+\vec{\tau}(\theta_{t_{n+1}})}{2}
\end{aligned}$$

where $\vec{\tau}(\theta) = (\cos\theta, \sin\theta)^T$.

In a first series of figures (3) the paths of the fibers for small stiffness ($\lambda = 100$) and different values of A are plotted. These plots are qualitatively the same as those for the original model. In all simulations we have chosen $b(r) = r$.

In a second series of figures (4) the case of moderate values of λ ($\lambda = 1$) is considered for different A. One clearly observes the smoother nature of the trajectories.

2.2 Comparison with numerical experiments

In this section the above results are qualitatively compared to the results of a numerical simulation of the full physical process developed in the software package FIDYST, see, for example [8, 9]. A more detailed quantitative comparison is planned for future work.

With FIDYST a single fiber in a spunbond process for nonwoven production is simulated. The fluid dynamic computations required for FIDYST are performed using the CFD tool FLUENT. For the simulation of the fiber dynamics the deterministic aerodynamic forces due to the mean stream and the stochastic forces due to turbulence are computed by means of the fluid dynamic results. The fiber is

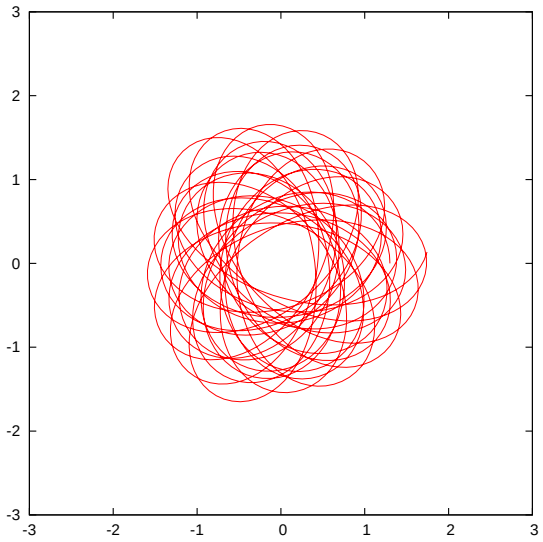

$\lambda = 100,\ A = \frac{\mu}{\lambda} = 0$

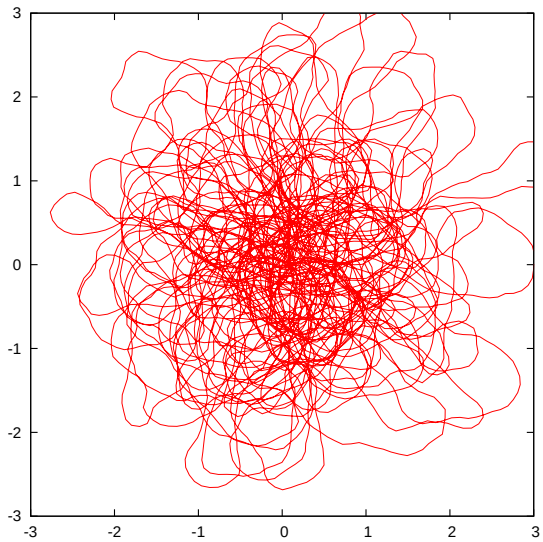

$\lambda = 100,\ A = \frac{\mu}{\lambda} = 1$

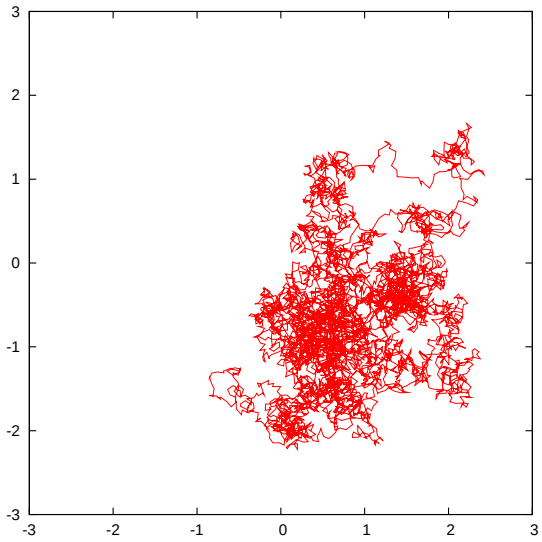

$\lambda = 100,\ A = \frac{\mu}{\lambda} = 10$

Figure 3: The smooth model near to the original model ($\lambda = 100$) for different values of A.

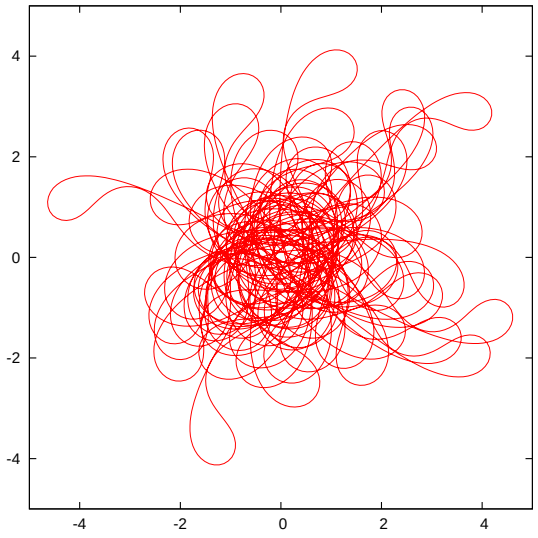

$\lambda = 1,\ A = \frac{\mu}{\lambda} = 0$

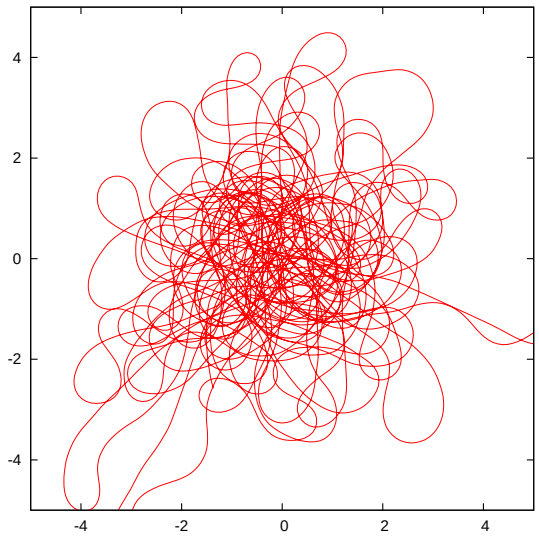

$\lambda = 1,\ A = \frac{\mu}{\lambda} = 1$

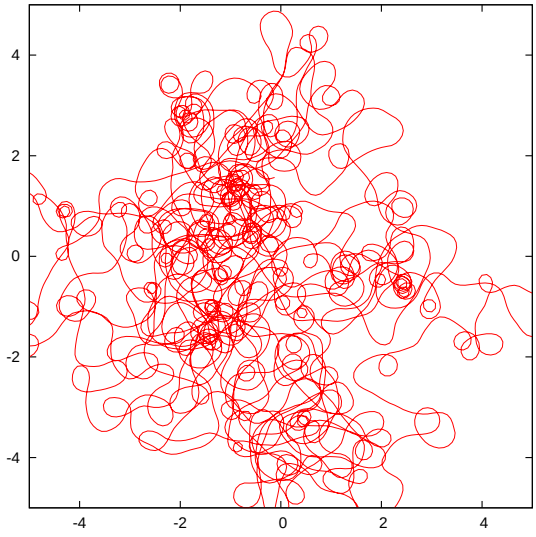

$\lambda = 1,\ A = \frac{\mu}{\lambda} = 5$

Figure 4: The smooth model with $\lambda = 1$ and different value of A

simulated for the full physical process between the exit nozzle and the conveyor belt including the lay-down process on the belt using a typical configuration of parameters. The fiber dynamics is given by a Newtonian equation of motion

$$\sigma\ddot{\vec{x}} = \partial_s(T(\partial_s\vec{x}) - EI\partial_{ssss}\vec{x} + f^{grav} + f^{air}$$

$$\|\partial_s\vec{x}\| = 1,$$

where the vector $\vec{x}(s,t)$ denotes the central line of the fibre.

Here, σ denotes the line density, T is a Lagrange parameter, I is the geometrical moment of inertia and E is the elasticity module. f^{grav} describes the influence of gravity and $f^{air} = f^{air}_{det} + Df^{air}_{stoch}$ give the deterministic and stochastic aerodynamic forces. In the present simulations the conveyor belt velocity is zero and a fixed distance between the nozzle and the conveyor belt is assumed. The inlet velocity of the fiber at the nozzle and the fiber length are also fixed. Only the fiber on the conveyor belt is shown. In the follwoing simulations we change the paramter E abd D.

In Figure 5 (upper left) a reference simulation is shown using an elasticity module $E = E_{ref}$ and a stochastic force with the parameter $D = D_{ref}$.

In Figure 5 (upper right) the stochastic forces are reduced by the factor 0.6, i.e. $D = 0.6D_{ref}$, leading to a more compact fiber lay-down.

Figure 5 (lower left) shows simulations with the original stochastic force and an increased elasticity module $E = 100E_{ref}$. This modification leads to larger loops of the fiber.

Figure 5 (lower right) finally shows results for reduced stochastic forces and increased elasticity module.

The paths in the upper two figures in Figure 5 showing a physical situation with moderate elasticity module E are qualitatively well approximated by simulations of the above stochastic model with values of A of size 3 and 2 and values of λ of size 5.

The paths in the lower two figures in Figure 5 showing situations with large elasticity module E. are qualitatively well approximated by simulations of the above model with values of A as above and values of λ of size 1.

3 Summary and Conclusions

In the present paper we did remove a drawback of the model developed in [2], i.e. the non-differentiability of the paths of the process. A model with smoother trajectories is developed by introducing a relaxation approximation. This is equivalent to an approximation of the White-noise process involved in the original model by an Ohrnstein-Uhlenbeck process. The relations of the different models are investigated analytically looking at different scalings and using diffusion approximations. We

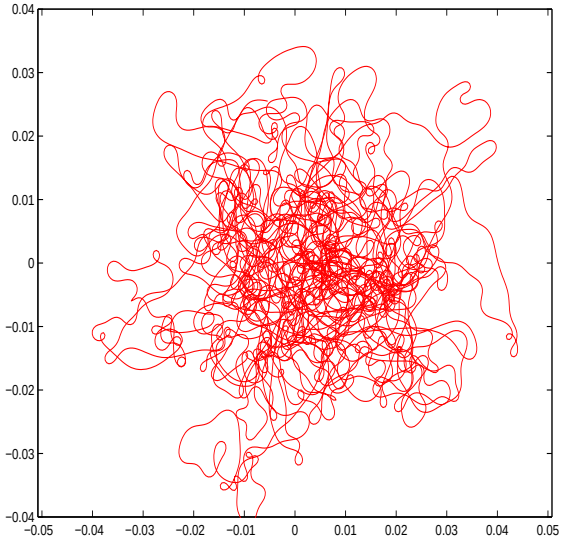

$D = D_{ref},\ E = E_{ref}$

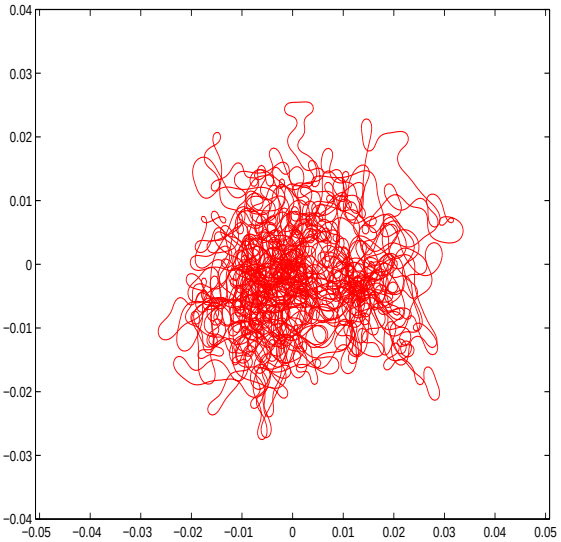

$D = 0.6D_{ref},\ E = E_{ref}$

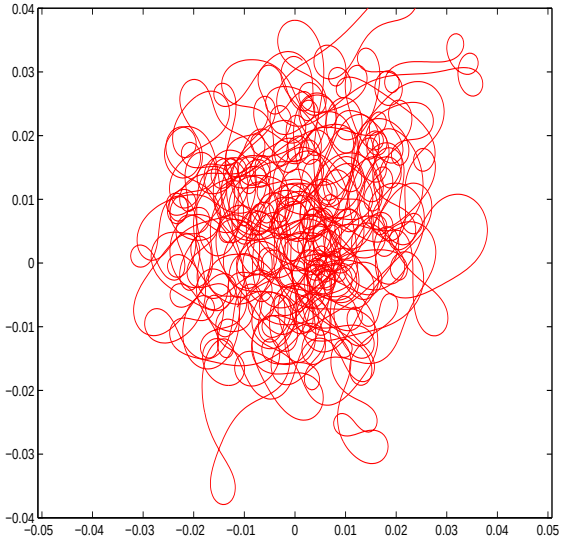

$D = D_{ref},\ E = 100E_{ref}$

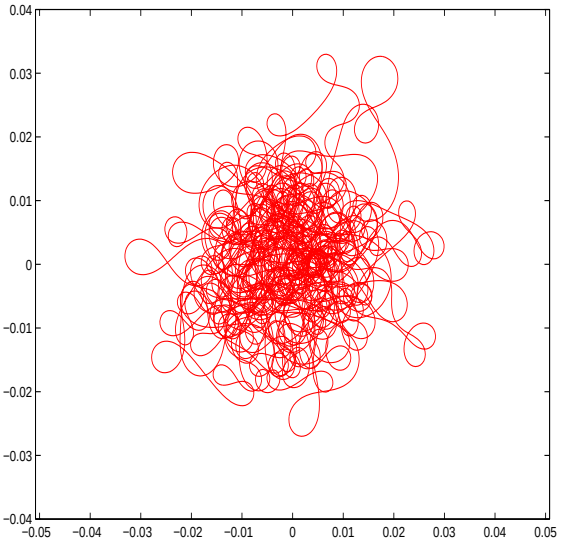

$D = 0.6D_{ref},\ E = 100E_{ref}$

Figure 5: Experimental results with small stochastic force (upper right), large elasticity module (lower left) and small stochastic force and large elasticity module (lower right).

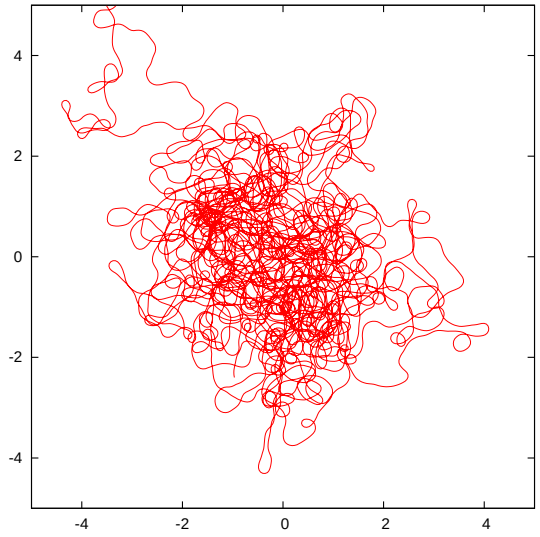

$\lambda = 5,\ A = \dfrac{\mu}{\lambda} = 3$

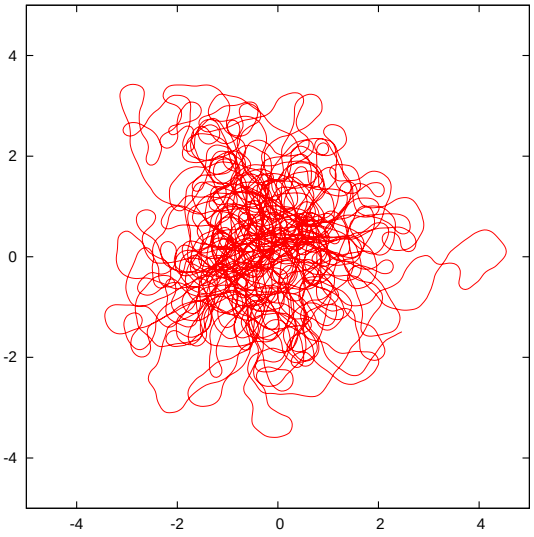

$\lambda = 5,\ A = 2$

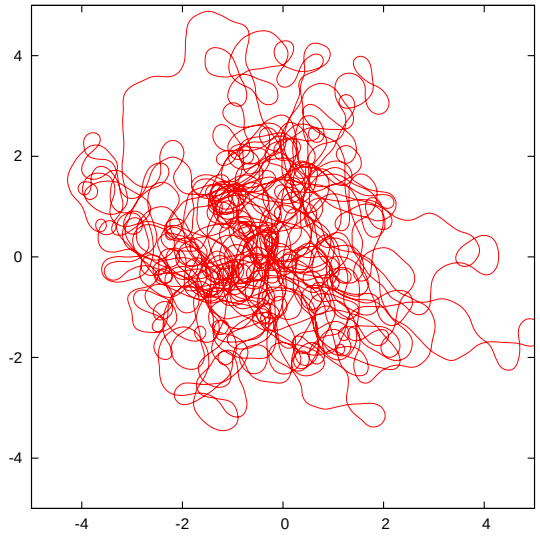

$\lambda = 2,\ A = 3$

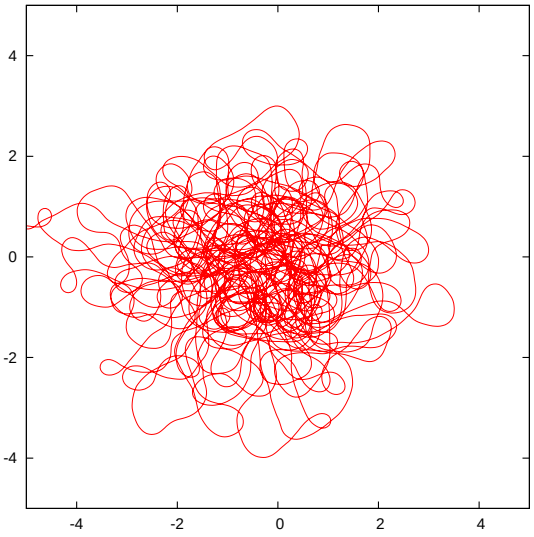

$\lambda = 2,\ A = 2$

Figure 6: The approximation of the experimental result using the smooth model.

also included a qualitative numerical comparison of the paths of the models for different parameters. The results show the improvement of the approximation of the paths compared to the original model.

Future work will be, in particular, devoted to the identification of the parameters μ and λ in the smooth model using data generated by the simulation of the full fibre spinning process.

Appendix

Proof of Proposition 1.2. Let's take the Fokker-Planck equation associated with the equation (1) using the rescaling given by (8) :

$$\varepsilon\partial_t f^\varepsilon + \vec{\tau}(\alpha)\cdot\nabla_{\vec{x}} f^\varepsilon + \partial_\alpha\left(b(r)\sin(\alpha-\phi)f^\varepsilon\right) = \frac{A^2}{2\varepsilon}\partial_{\alpha^2} f^\varepsilon. \tag{25}$$

Using a Hilbert expansion for f^ε ($f^\varepsilon = f^0 + \varepsilon f^1 + \dots$), we find :

$$\varepsilon^{-1} \quad : \quad \partial_{\alpha^2} f^0 = 0,$$

that means $f^0(t,\vec{x},\alpha) = n^0(t,\vec{x})\,\frac{1}{2\pi}$. For the term in ε^0 we have:

$$\varepsilon^0 \quad : \quad \vec{\tau}(\alpha)\cdot\nabla_{\vec{x}} f^0 + \partial_\alpha\left(b(r)\sin(\alpha-\phi)f^0\right) = \frac{A^2}{2}\partial_{\alpha^2} f^1.$$

This equation can be explicitly solved since f^0 doesn't depend on α. Integrating twice in α, we have :

$$f^1 = \frac{2}{A^2}\frac{1}{2\pi}\left[-\vec{\tau}(\alpha)\cdot\nabla_{\vec{x}} n^0 - b(r)\cos(\alpha-\phi)\,n^0\right].$$

Finally, integrating the original equation for f^ε in α, we have :

$$\varepsilon^{-1} \quad : \quad \varepsilon\partial_t n^\varepsilon + \nabla_{\vec{x}}\cdot\left(\int_0^{2\pi}\vec{\tau}(\alpha)\,f^\varepsilon\,d\alpha\right) = 0.$$

Replacing f^ε by its Hilbert expansion, we have :

$$\partial_t n^0 + \nabla_{\vec{x}}\cdot\left(\int_0^{2\pi}\vec{\tau}(\alpha)\,f^1\,d\alpha\right) = O(\varepsilon). \tag{26}$$

Then by some easy computations, we can evaluate the integral :

$$\begin{aligned}\int_0^{2\pi}\vec{\tau}(\alpha)\,f^1\,d\alpha &= \frac{1}{2\pi}\frac{2}{A^2}\int_0^{2\pi}\left[\nabla_{\vec{x}} n^0\,\vec{\tau}(\alpha)\otimes\vec{\tau}(\alpha) - b(r)\cos(\alpha-\phi)\vec{\tau}(\alpha)\,n^0\right]d\alpha \\ &= -\frac{1}{\pi A^2}\left[\nabla_{\vec{x}} n^0\,\pi \;-\; b(r)n^0\int_0^{2\pi}\cos(\alpha-\phi)\vec{\tau}(\alpha)\,d\alpha\right].\end{aligned}$$

Or we can develop the cosines of $(\alpha - \phi)$, this gives :

$$\begin{aligned}\int_0^{2\pi} \cos(\alpha-\phi)\vec{\tau}(\alpha)\,d\alpha &= \int_0^{2\pi} (\cos\alpha\cos\phi + \sin\alpha\sin\phi)\vec{\tau}(\alpha)\,d\alpha \\ &= \pi \begin{pmatrix} \cos\phi \\ \sin\phi \end{pmatrix}.\end{aligned}$$

Therefore, we have :

$$\int_0^{2\pi} \vec{\tau}(\alpha)\, f^1\, d\alpha = -\frac{1}{A^2}\,[\nabla_{\vec{x}} n^0 \; - \; b(r) n^0 \vec{\tau}(\phi)].$$

Now if we go back to equation (26), we have at the limit ε goes to zero :

$$\partial_t n^0 - \frac{1}{A^2}\nabla_{\vec{x}} \cdot \left(b(r)\vec{\tau}(\phi)\, n^0\right) = \frac{1}{A^2}\,\Delta_{\vec{x}} n^0.$$

□

Acknowledgments : Grateful acknowledgement is due to Egide for its financial support.

References

[1] T. Goetz, A. Klar, N. Marheineke, and R. Wegener, *A stochastic model for the fiber lay-down process in the nonwoven production*, SIAM J. Appl. Math., (2007). In press

[2] L. L. Bonilla, T. Goetz, A. Klar, N. Marheineke, R. Wegener *Hydrodynamic limit of a Fokker Planck equation describing fiber lay down processes*, SIAM J. Appl. Math., (2007). In press

[3] P. Degond, S. Motsch, *Large-scale dynamics of the Persistent Turning Walker model of fish behaviour*, preprint

[4] L. Arnold, *Stochastic Differential equations*, Springer, 1978.

[5] B. Oksendal, *Stochastic differential equations*, Springer-Verlag, 1992.

[6] M. Grothaus and A. Klar, *Ergodicity and rate of convergence for a non-sectorial fiber lay-down process*, preprint

[7] A. Klar, P. Reuterswärd, M. Seaïd *A semi-Lagrangian method for a Fokker-Planck equation describing fiber dynamics*, preprint

[8] N. Marheineke, R. Wegener, *Fiber dynamics in turbulent flows: General modeling framework*, SIAM J. Appl. Math. 66(5), 1703-1726, 2006.

[9] N. Marheineke, R. Wegener, *Fiber dynamics in turbulent flows: Specific Taylor drag*, SIAM J. Appl. Math., to appear